Photovoltaic Capacity Additions: The optimal rate of deployment with sensitivity to time-based GHG emissions

by

Dwarakanath Triplican Ravikumar

A Thesis Presented in Partial Fulfillment
of the Requirements for the Degree
Master of Science

Approved November 2013 by the
Graduate Supervisory Committee:

Thomas Seager, Co-Chair
Matthew Fraser, Co-Chair
Mikhail Chester
Parikhit Sinha

ARIZONA STATE UNIVERSITY

December 2013

ABSTRACT

Current policies subsidizing or accelerating deployment of photovoltaics (PV) are typically motivated by claims of environmental benefit, such as the reduction of CO_2 emissions generated by the fossil-fuel fired power plants that PV is intended to displace. Existing practice is to assess these environmental benefits on a net life-cycle basis, where CO_2 benefits occurring during use of the PV panels is found to exceed emissions generated during the PV manufacturing phase including materials extraction and manufacture of the PV panels prior to installation. However, this approach neglects to recognize that the environmental costs of CO_2 release during manufacture are incurred early, while environmental benefits accrue later. Thus, where specific policy targets suggest meeting CO_2 reduction targets established by a certain date, rapid PV deployment may have counter-intuitive, albeit temporary, undesired consequences. Thus, on a cumulative radiative forcing (CRF) basis, the environmental improvements attributable to PV might be realized much later than is currently understood. This phenomenon is particularly acute when PV manufacture occurs in areas using CO_2 intensive energy sources (e.g., coal), but deployment occurs in areas with less CO_2 intensive electricity sources (e.g., hydro). This thesis builds a dynamic Cumulative Radiative Forcing (CRF) model to examine the inter-temporal warming impacts of PV deployments in three locations: California, Wyoming and Arizona. The model includes the following factors that impact CRF: PV deployment rate, choice of PV technology, pace of PV technology improvements, and CO_2 intensity in the electricity mix at manufacturing and deployment locations. Wyoming and California show the highest and lowest CRF benefits as they have the most and least CO_2 intensive grids, respectively. CRF payback times are longer

than CO_2 payback times in all cases. Thin film, CdTe PV technologies have the lowest manufacturing CO_2 emissions and therefore the shortest CRF payback times. This model can inform policies intended to fulfill time-sensitive CO_2 mitigation goals while minimizing short term radiative forcing.

DEDICATION

To Thara, Miyuki, Dhiren, my in-laws and Mother Nature

ACKNOWLEDGMENTS

I would like to thank my committee members for their guidance and continued support. Dr. Seager was relentless in his efforts to make me look at the big picture (and not just be the compulsive fact-finder) and improve my exposition in the thesis. His advice and inputs on research and presenting ideas that change the prevailing ways of designing and conducting Photovoltaic LCAs have been an inspiration and have constantly pushed me to work beyond my comfort zone. Dr. Fraser has been extremely helpful with his advice and mentoring and has also funded my travel to research conferences through QESST. The feedback received in these conferences has greatly improved the analysis used in this thesis. Dr. Chester has been a great mentor right from the incipient stages of this thesis. His keen eye for detail and his LCA class have been of great value in strengthening the fundamentals and methods presented in this thesis. Dr. Sinha has been generous with his time and was an involved and enthusiastic industry partner. His insights on current PV industry practices and contemporary research methods have been critical in improving the quantitative modeling in this thesis. I would like thank to Ben, Valentina, Susan, Andrew and Dan from the Sustainable Energy and Environmental Decision Science (SEEDS) studio at ASU for their valuable feedback. I would like to acknowledge my academic mentors in India, Dr. Deepak Malghan, Dr. Varadharajan Sridhar, Dr. Asha Bhandarkar, and my good friend Gabriel Grant for advising me during the transition stage of becoming a graduate student and being liberal with their time.

This thesis is based upon work primarily supported by the National Science Foundation (NSF) and the Department of Energy (DOE) under NSF CA No.EEC-1041895. Any opinions, findings and conclusions or recommendations expressed in this material are those of the author and do not necessarily reflect those of NSF or DOE.

TABLE OF CONTENTS

APPENDIX

LIST OF TABLES

LIST OF FIGURES

Figure Page

CHAPTER 1

INTRODUCTION

PV capacities have increased from 277 MW in 2000 to 32,223 MW in 2012 and are projected to further grow at the international, national and state levels [1-3]. The share of PV electricity is projected to increase to around 11% of the total electricity generated worldwide by 2050 [4]. The Sun Shot initiative launched by the US Department of Energy seeks to deploy 632 GW by 2050 which is significantly greater than the cumulative installed capacity of 2.5GW in 2010 [3, 5]. The primary motive of increased PV deployments is to reduce dependence on fossil fuels for electricity generation and prevent the global warming impacts of the associated GHG emissions [4, 6]. This large scale increase in PV deployments involves upfront CO_2 emissions during the raw material extraction, purification and PV manufacturing stages which is gradually offset by the CO_2 avoided as PV electricity displaces grid electricity generated from fossil fuels. Due to this temporal CO_2 trade-off and the rapid increase in worldwide PV capacity additions, the magnitude of upfront PV manufacturing CO_2 emissions can temporarily increase global warming impacts. The short term global warming impacts of these CO_2 flows should be evaluated for time frames defined by climate policy for reducing GHG emissions to prevent a 2 to 4 degree Celsius global temperature rise. The typical time frames identified by climate goals is thirty to fifty years [7].

Life Cycle Assessment (LCA) is the preferred framework to evaluate such environmental impacts over the PV lifecycle. LCAs quantify the environmental impacts of the material and energy flows for each stage of the PV lifecycle and ensure that impacts are not shifted from one life cycle stage to another [8]. Energy payback time (EPBT) is the primary metric used in PV LCAs to measure temporal energy trade-offs over the PV lifecycle [9-11]. EPBT is a ratio of the total energy produced by a PV module in the use phase and the energy invested in manufacturing a PV system. EPBT does not consider the CO_2 footprint of the energy used to manufacture the PV modules or the CO_2 intensity of the grid electricity that is displaced at the deployment location. EPBT does not quantify the CO_2 flows emitted and avoided during the PV manufacturing and use phase, respectively, and therefore cannot be used to measure the global warming impacts of PV deployments. PV LCAs have also relied on the 'grams/kWh' metric to compare the CO_2 footprint of PV electricity with other traditional electricity sources [9, 12-14]. This metric is determined by allocating the PV lifecycle CO_2 emissions over the total electricity generated during the use phase of the PV modules. However, by ignoring the CO_2 footprint of the electricity displaced during the use phase of the PV module, this metric does not quantify the CO_2 flows avoided during the use phase of the PV module. Therefore, existing PV LCA standards [15] and studies [13, 14, 16, 17] do not measure temporal trade-off of CO_2 over the PV lifecycle and cannot measure the corresponding short-term global warming impacts.

The global warming potential of a CO_2 emission is a non-linear function of the atmospheric residence time of CO_2 (Equation (2)) and can be measure using the Cumulative Radiative Forcing (CRF) which was developed by IPCC [18]. A limited number of LCA studies have used the CRF metric to incorporate non-linear warming impacts of GHG flows over a product's lifecycle. Kendall and Price provided a method to quantify the trade-offs between increased upfront CO_2 emissions required to manufacture light weight fuel efficient vehicles and the decreased CO_2 emissions due to the higher fuel efficiency of these vehicles [19]. This study used a CRF based time correction metric to account for actual GWP impacts when the vehicle's manufacturing and end of life emissions are averaged over the total distance travelled during the life time. Another study developed a correction factor which accounts for the difference in CRF impacts when CO_2 emissions attributed to land use changes at the start of biofuels life cycle is amortized over a longer time horizon [20]. Kendall developed a correction factor based on the difference in CRF impacts of temporally separated CO_2 emissions occurring over different stages of a product's life cycle [21]. Chang and Kendall have quantified the difference in payback times for CO_2 and CRF when the CO_2 emitted while constructing a high speed rail (HSR) system is gradually offset by the CO_2 emissions avoided when HSR displaces road and air travel [22].

The CRF based correction factors developed in these studies are restricted to transportation and biofuel LCAs and are not directly applicable to PV LCAs. The scenarios modeled involve a single upfront emission (e.g., land use change for biofuels, construction of transportation infrastructure) which is offset by CO_2 emissions that are avoided later in time. There is no distinct one time emission when PV systems are deployed because PV systems installations do not happen at once but are staggered over a period of time. The CO_2 avoided each year is a function of the cumulative PV capacity added until that year. Further, technology improvements, grid CO_2 intensities at the manufacturing and deployment locations and the choice of PV technology further introduce complexity in quantifying the CRF impacts of PV system deployments. Upfront PV manufacturing CO_2 emissions and the CO_2 avoided over the use phase of the PV system are a function of these dynamic factors.

This study has developed a framework (Figure 2) that incorporates these factors and measures the CO_2 and CRF impacts of California's PV policy targets.

Cumulative Radiative Forcing (CRF)

The CRF impact of a pulse CO_2 emission is determined by the radiation that it absorbs when it decays in the atmosphere before it is completely sequestered. This atmospheric decay of CO_2 is defined by the Bern carbon cycle model [18] and is given by

$$c(t) = 0.217 + (0.259 * e^{-t/172.9}) + (0.338 * e^{-t/18.51}) + (0.186 * e^{-t/1.186}) \qquad (1)$$

where c(t) is the CO_2 that is resident in the atmosphere after 't' years have elapsed since the unit pulse of CO_2 was emitted. As the CO_2 decays in the atmosphere it traps radiation which gives rise to the greenhouse effect. This radiation imbalance caused by a decaying pulse of CO_2 is measured using the CRF metric [18]. The CRF (in watts/m2) caused by a CO_2 pulse decaying over a time period of TH years is given by

$$CRF = \int_0^{TH} \left(a_c \times c(t)\right) dt \qquad (2)$$

where ac is radiative efficiency of CO_2 and is defined as follows

$$a_c = 5.35 * \log\left(C \div Co\right) \qquad (3)$$

where Co is the initial CO_2 concentration in the atmosphere and C is the concentration in the atmosphere after the event which causes the perturbation. Based on IPPC's approach, a_c is assumed to be constant at 1.4135×10^{-5} by setting C_o at 378 ppm and C at 379 ppm after a +1 ppm perturbation [18].

Time Sensitivity of CRF impacts

From Equation (2) it can be inferred that the CRF impacts of a CO_2 emission is dependent on the year in which the emission occurs and the atmospheric residence time over which the impacts are calculated (TH). The time sensitive CRF impacts of CO_2 emissions over a ten year horizon is depicted in Figure 1. The time horizon chosen is consistent with the 10 year horizon of California's Solar initiative whose CRF impacts are modeled in later sections.

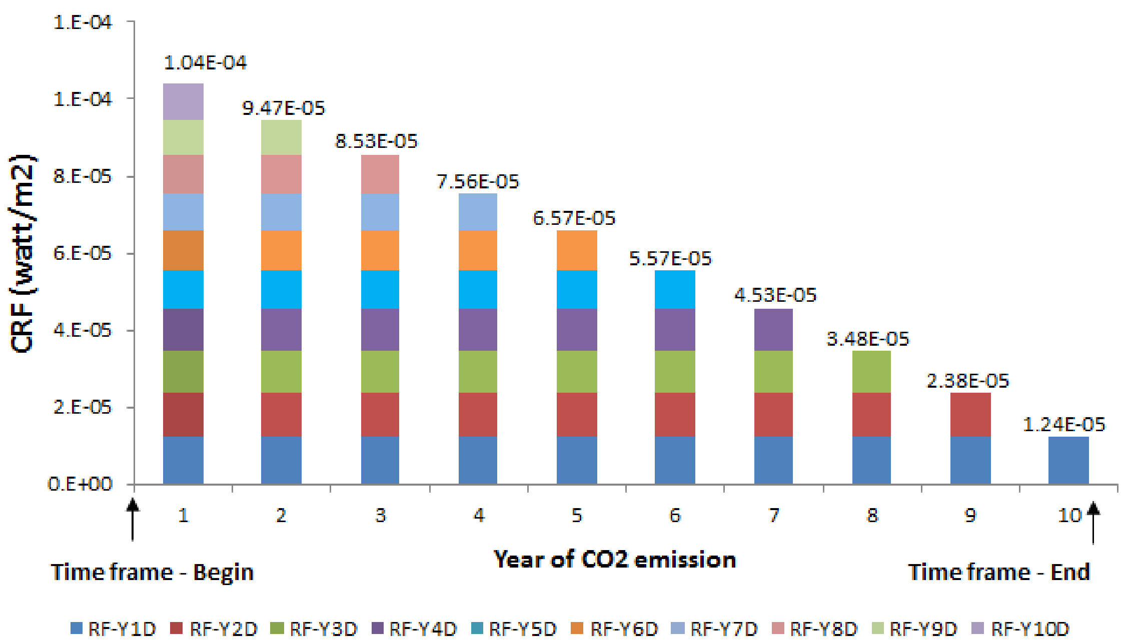

Figure 1 CRF impacts of CO_2 emissions over a 10 year time horizon. The CRF impacts of one Kg of CO_2 emitted in a particular year 'n' is measured over a time period of (10-n) years. The impact is depicted by the height of the multi-colored bar

in that year. The colored blocks within the multi-colored bar represent Radiative Forcing (RF) components that contribute to the CRF. For example, if one Kg of CO_2 was emitted in year 5 then the CRF impact is 6.57E-05 watt/m2 and it consists of six RF components represented by the six colored blocks. The six colored blocks represent the annual RF impacts for each of the six years that the CO_2 decays (from the beginning of year 5 to end of year 10). For example, the red block (RF – Y2D in the multi-color bar in year 5) represents the radiative forcing as CO_2 decays during the 2nd year after emission.

Therefore, the CRF metric provides a time sensitive quantitative measure of the environmental impacts of a pulse of CO_2 emission. This study designs a CRF based framework to evaluate the time sensitive environmental impacts of CO_2 flows during the PV lifecycle. Earlier CO_2 emissions in the PV lifecycle will be will be assigned a higher weightage when compared to a later emission due to higher CRF impacts. For example, let 100 grams of CO_2 be emitted when a PV module is manufactured and deployed in year one and let this PV module displace 30 grams of CO_2 for every subsequent year. The 100 gram emission is assigned the year 1 weight and the 30 grams of CO_2 that are subsequently avoided are assigned the weights from year 2 to 10. The net CRF benefit at the end of 10 years is the difference between the avoided and emitted CRF and is 4.4E-06 watts/m2. The calculation for CRF weights are explained in Appendix A.

The time sensitive CRF impacts of PV deployments will depend on the timing of CO_2 emitted and avoided during the PV lifecycle and there is a need to determine the parameters that impact the magnitude and timing of the CO_2 flows to minimize the CRF impacts.

Magnitude of CO_2 emitted and avoided over PV lifecycle

The following figure depicts the PV supply chain and technology parameters that impact the magnitude of the CO_2 flows over the PV lifecycle

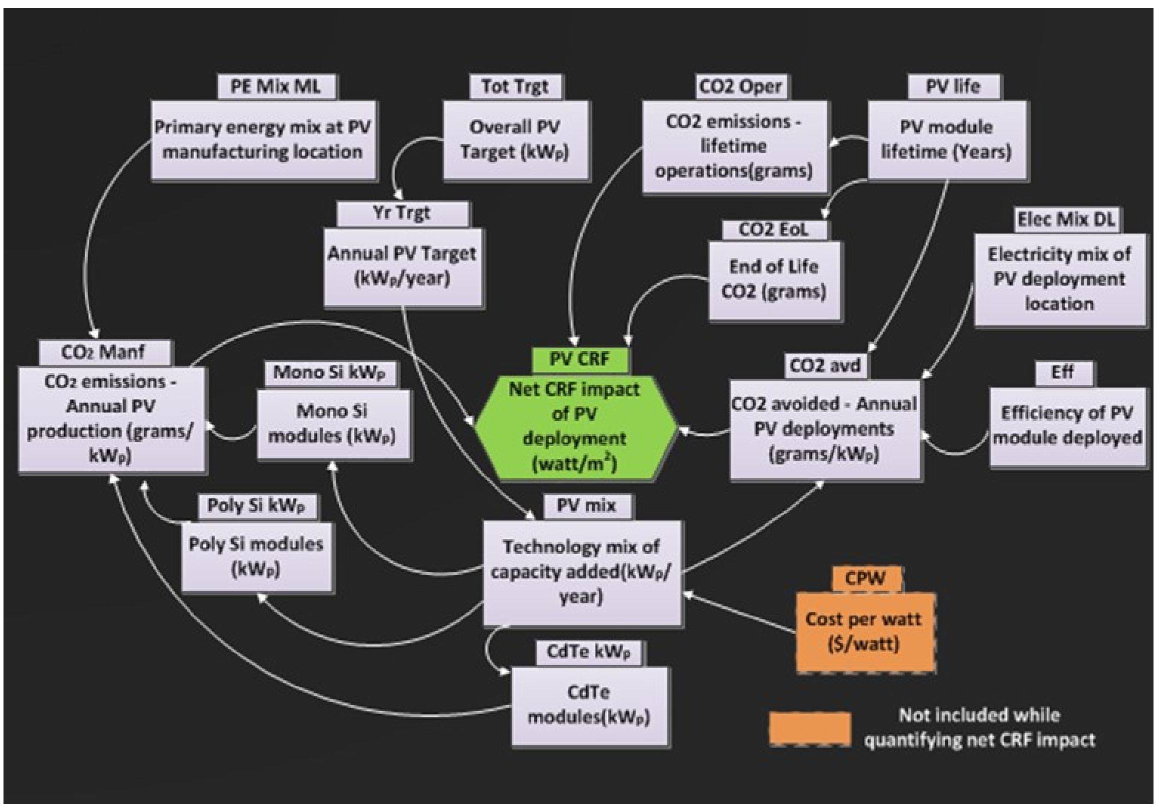

Figure 2 PV supply chain and technology parameters that impact the magnitude of CO_2 emitted and avoided over the PV lifecycle

The annual PV target (“Yr Trgt”) can be fulfilled through a mix of mono crystalline Silicon, poly crystalline Silicon and thin film CdTe (“PV mix”, “CdTe kWp”, “Mono Si kWp” , “Poly Si kWp”). These three PV technologies have different manufacturing energy requirements. The manufacturing energy requirements per square meter of the Mono Si and CdTe module are the highest and lowest, respectively [9]. The CO_2 emitted over the manufacturing phase of the PV lifecycle (“CO_2 Manf”) is dependent on the primary energy mix at the manufacturing location (“PE Mix ML”) and the manufacturing energy requirements of the PV technology. Mono Si is the most CO_2 intensive to manufacture ($MCI_{china\ mono\ si}$ in Table 2) as the manufacturing energy requirements are the highest and mono Si modules are primarily manufactured in China where coal contributes to around 67% of the primary energy mix. Similarly, CdTe is the least CO_2 intensive to manufacture ($MCI_{Malaysia\ CdTe}$ in Table 2) as the manufacturing energy requirements are the lowest [9] and they are primarily manufactured in Malaysia which has lower CO_2 footprints for the primary energy than China. The environmental benefit of PV deployments is determined by the CO_2 emissions avoided annually (“CO_2 avd”) as PV electricity offsets grid electricity generated from fossil fuels. “CO_2 avd” is dependent on the CO_2 intensity of the electricity grids at the deployment location (“Elec Mix DL”) and the efficiency of the modules deployed (“Eff”). For a fixed deployment area, the electricity generated by the PV system is directly proportional to the module efficiency and this determines the grid CO_2 that is displaced at the deployment location. The CO_2 emitted while maintaining, decommissioning and recycling PV modules (“CO_2 Oper”, “CO_2 EoL”) is assumed to be 10% of the overall CO_2 emitted to manufacture PV modules [23]. The magnitude and timing of "CO_2 Manf" and "CO_2 avd" determine the net CRF impact ("PV CRF") over the policy time frame.

Timing of CO_2 emitted and avoided over PV lifecycle

The decision to increase PV deployments earlier on during the policy time frame or to postpone (or stagger) deployments to a later date will determine the timing of the CO_2 emitted and avoided. For example, consider the following strategies that can be adopted to meet a target of 1 GW over a 10 year time period

Strategy 1: 0.4 GW in year 1 and 0.1 GW over the next 6 years

Strategy 2: 0.1 GW over the first 6 years and 0.4 GW during the 7^{th} year

Strategy 1 leads to larger upfront manufacturing emission as a higher PV capacity is deployed earlier on when compared to the staggered approach in strategy 2. In strategy 1, earlier and larger upfront PV manufacturing emissions not only increase the initial CRF cost (as explained in Figure 1) but also increase the CRF benefits by displacing more fossil fuel electricity during the PV module's use phase.

In case of strategy 2, upfront PV manufacturing emissions are comparatively lower as only 0.1 GW is deployed from year 1 to 6. Thus, manufacturing emissions occurring later in time decreases the PV manufacturing CRF cost of Strategy 2. However, Strategy 2 also incurs a "waiting cost" as the delayed deployment implies that grid electricity, which would have been offset by PV electricity, continues to be generated and used.

At any given point of time, the decision to deploy a larger PV capacity upfront ('Front Load') or postpone PV capacity additions to a future date ('Back Load') will determine the timing of the CO_2 emitted and avoided and therefore influence the CRF impacts. The

CO_2 trade-off, which influences the CRF impacts, for the front loading and back loading strategy are shown in Figure 3 and Figure 4.

Timing of CO_2 emissions for Front Loading strategy

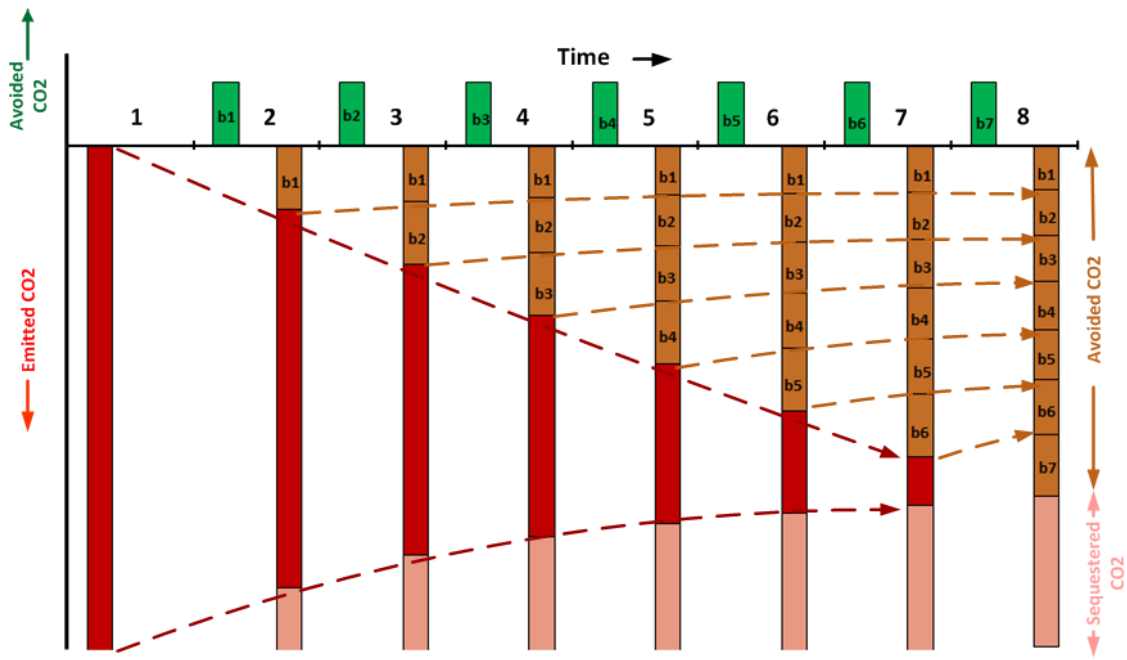

Figure 3 CO_2 flows for the Front Loading Strategy. The positive Y axis represents CO_2 benefits and the negative Y axis the CO_2 costs of deploying PV systems. The PV system is deployed in year 1 and the corresponding PV manufacturing CO_2 emission is represented by the solid red bar. Every year, a portion of this emitted CO_2 is sequestered in the atmosphere (refer equation(1)) and this is represented by the pink bar. The solid green bars from year 2 onwards (e.g. b1, b2, b3) represent the CO_2 emissions avoided as PV electricity offsets grid electricity. The CO_2 emissions avoided are deducted from the red bar and this represented by the solid brown bars. The deductions are cumulative, for example in year 4, the decayed values of year 1 and 2 benefits (b1 and b2) and year 3 benefits (b3) is deducted from the CO_2

emitted in year 1.The hashed brown line represent the decay the avoided CO_2 would have undergone had it been emitted. The hashed red arrows represent the gradual decrease in the initial PV manufacturing CO_2 emission. In year 8, when the solid red bar reduces to zero, the total CO_2 emitted in year 1 is "paid back" through the CO_2 avoided.

The PV system is deployed in year 1 and the PV manufacturing CO_2 emission is represented by the red bar and is assumed to be emitted at the point of deployment in year 1. The height of this red bar is the product of the PV capacity deployed and the CO_2 intensity of the manufactured PV modules.

$$mCO2_t = \sum_{i=monoSi,PolySi,CdTe} W_{t\_i} \times MCI_{t\_i} \quad (4)$$

where

- m CO_2 t = PV manufacturing CO_2 emissions in year 't' (grams)
- i = PV technology deployed. Three types of PV technology are considered: Mono Si, Poly Si, CdTe
- W_{t_i}= capacity of a particular PV technology 'i' deployed in the year 't' (Wp)
- MCI_{t_i} = CO_2 intensity of the manufactured PV modules in the year 't' for technology 'i' (grams/kWp)

Once emitted, the manufacturing CO_2 emission is gradually sequestered (defined by equation(1)) and this sequestered CO_2 is represented by the pink bar. The environmental benefit of deploying a PV module is the CO_2 avoided every year as PV electricity displaces electricity generated from fossil fuels. The avoided CO_2 is represented by the solid green bars and can be mathematically defined as

$$aCO2_t = \sum_{i=monoSi,PolySi,CdTe} \left(\sum_{k=1}^{t} W_{k\_i} \right) \times pr \times irr \times (1-op) \times (1-tl) \times DGI_{t\_i} \times apd \qquad (5)$$

where

- a CO_2 n = CO_2 emissions avoided in year ‘t’ (grams)
- W_{k_i}=cumulative PV capacity addition till the year t (Wp)
- pr = performance ratio, the ratio between the AC power generated to the rated DC power.
- Irr = solar irradiation at the deployment location (kWh/Wp/year)
- op= ratio of energy spent on the operations and maintenance of the PV module to the total energy generated by the PV module.
- tl = transmissions losses during electricity distribution.
- DGI_{t_i} = CO_2 intensity of the grid at the deployment location, .i.e. CO_2 emitted per unit of electricity generated at the deployment location in the year ‘t’ for technology ‘i’ (grams/kWh)
- apd=annual performance degradation in the PV module

Every year the avoided CO_2 is deducted from the initial CO_2 emitted and this is depicted using solid brown bars. The CO_2 benefits of a PV module accrue over a period of time and it is only in the 8^{th} year that there is a net benefit when the magnitude of the solid red bar becomes zero.

Timing of CO_2 emissions for Back Loading strategy

The timing of the CO_2 emitted and avoided for the "back loading" strategy is depicted in Figure 4

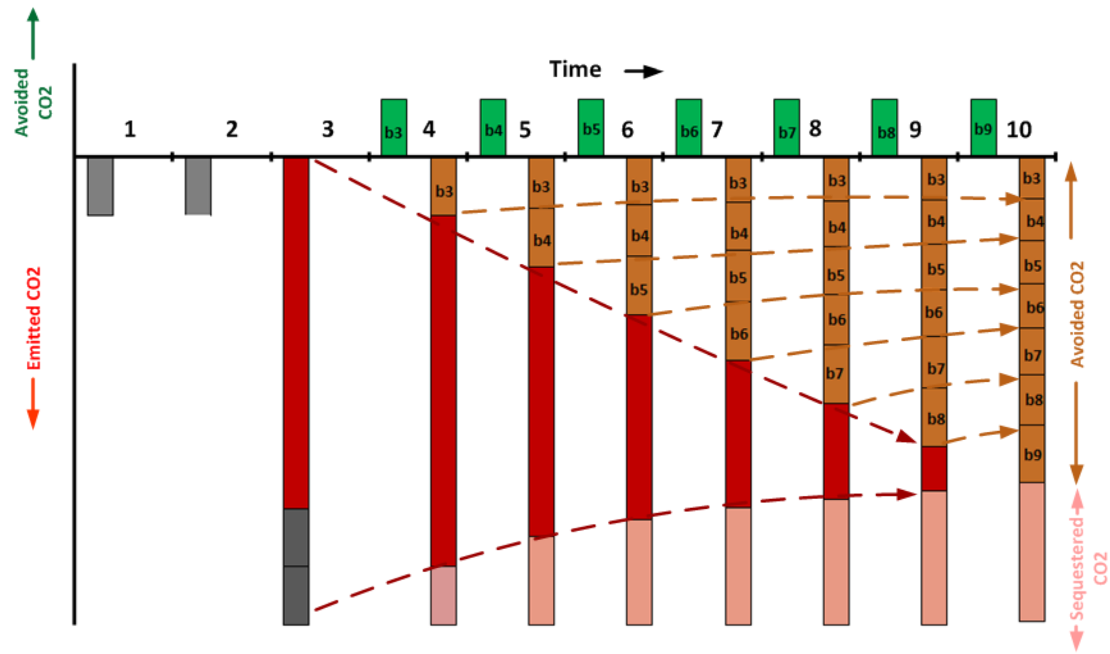

Figure 4 CO_2 flows for the Back Loading Strategy. The PV system is deployed in year 3 and the grey bars in year 1 and 2 represent the CO_2 emissions due to continued reliance on grid electricity. The other depictions are similar to Figure 3.

In this example, the PV capacity 'C' is deployed in year 3 and there is an additional CO_2 emission in year 1 and 2 due to the continued generation of electricity from fossil fuels. This is depicted by grey bars in year 1 and 2. The magnitude of year 1 and 2 emissions are equal to the magnitude of the CO_2 emissions avoided from year 3 onwards as these are equal to the electricity that the PV capacity 'W3' displaces every year (equation (5)). The benefit of back loading is that PV technology improves over this wait period and this is modeled by increasing module efficiencies and reduced manufacturing energy requirements. The remaining aspects of Figure 4 are similar to Figure 3. CO_2 emissions due to back loading can be mathematically defined as

$$bCO2_t = \sum_{i=monoSi,PolySi,CdTe} \left(C - \sum_{k=1}^{t} W_{k\_i} \right) \times pr \times irr \times (1-op) \times (1-tl) \times DGI_{t\_i} \times apd \qquad (6)$$

The terms in equation (6) are similar to the terms defined in equation (5)

Optimization framework for PV deployment

This study has built an optimization framework which incorporates the PV supply chain and technology factors that impact the magnitude of CO_2 emissions and the deployment strategy (Front loading and Back loading) that determines the timing of the CO_2 emissions. The optimal PV deployment has the minimal CRF impacts measured over a ten year time frame that is defined in California's solar initiative [24]. The optimization framework used the following CRF categorization of to determine the optimal PV deployment strategy

- Avoided CRF ($CRF_{av}(t)$): CRF avoided in a year due to PV electricity displacing electricity generated from fossil fuels. This is the CRF associated with the avoided CO_2 emissions (solid green bars in Figure 4) that is defined in equation(5). The optimization framework will treat this as a CRF benefit that has to be maximized. $CRF_{av}(t)$ can be mathematically defined as

$$CRF_{av}(t) = a_c \times \sum_{t=1}^{n} (aCO2_t \times k_t) \qquad (7)$$

where k_t is discussed in Figure 1, a_c is defined in equation (3), $aCO_{2\,t}$ is defined in equation (5).

- PV manufacturing CRF ($CRF_{mnf}(t)$): CRF due to manufacturing the PV capacity that was deployed in a particular year. This is the CRF associated with the PV manufacturing CO_2 (solid red bar in Figure 4) that is defined in equation(4). The optimization framework will treat this as a CRF cost that has to be minimized. $CRF_{mnf}(t)$ can be mathematically defined as

$$CRF_{mnf}(t) = a_c \times \sum_{t=1}^{n} \left(mCO2_t \times k_t \right) \qquad (8)$$

where $mCO_{2\,t}$ is defined in equation (4).

- Backloading CRF ($CRF_{bl}(t)$): CRF that was not avoided due to the back loading of PV deployments. This is the CRF associated with the solid grey bars in Figure 4 that is defined in equation(6). The optimization framework will treat this as a CRF cost that has to be minimized. $CRF_{bl}(t)$ can be mathematically defined as

$$CRF_{bl}(t) = a_c \times \sum_{t=1}^{n} \left(bCO2_t \times k_t \right) \qquad (9)$$

where bCO_2 t is defined in equation (6)

The CRF impacts of PV deployment can be minimized by maximizing the following objective function which is dependent on the three CRF categories

$$Z = \sum_{t=1}^{n} CRF_{av(t)} - CRF_{mnf(t)} - CRF_{bl(t)} \qquad (10)$$

$CRF_{av}(t)$, $CRF_{mnf}(t)$ and $CRF_{bl}(t)$ are dependent on CO_2 emitted and avoided every year which is determined by the annual PV capacities deployed every year (Wt in equations

(4), (5) and (6)). Therefore, W_t is the decision variable that is optimized. Changing W_t will affect the three categories of CRF and will thus change Z.

The only constraint on W_t is that it should be less than the total PV target set by policy

$$\sum_{1}^{n} W_t \leq C \qquad (11)$$

The California Solar Initiative (CSI) has set a goal of adding 1940 MW of PV capacity between 2007 and 2016 [24]. 81 MW and 169 MW were deployed in 2007 and 2008 and therefore these values will be fixed [25]. The deployment of the remaining 1690 MW ('C') will be optimized between 2009 and 2016.

If the optimization results in a greater share of the total policy targets being deployed within the first five years (out of a total 10 years) then front-loading is the optimal strategy. Similarly, if a greater share of the total policy targets is deployed over the last five years then back-loading is the optimal strategy. The data assumptions for the optimization framework are explained in Appendix C.

CHAPTER 3

RESULTS

Optimal PV deployment strategy and CO_2 and CRF impacts

Along with California, the model was run for Arizona and Wyoming. These three states were chosen to study the change in the optimal deployment strategy for different grid CO_2 intensities at the PV deployment location. The share of fossil fuels in the electricity mix determines the grid CO_2 intensities in these states. China is assumed to be the manufacturing location for Mono and Poly Si modules as around 60% of the world's Si PV modules are manufactured in China and 11 among the top 15 PV module manufacturers are Chinese [2]. First solar is the only thin film PV manufacturer in the top 10 PV manufacturers worldwide [26]. Malaysia is assumed to be the manufacturing location for CdTe modules as 70% of First Solar's modules are produced in Malaysia [27]. The results for the optimal PV deployment strategy that minimizes the CRF impacts of deploying a PV capacity of 1940 MW across three states - California, Arizona and Wyoming- is depicted in Figure 5. Front loading is the optimal strategy across all the three states for any technology mix that is chosen when the CRF impacts are considered from 2007 to 2017.

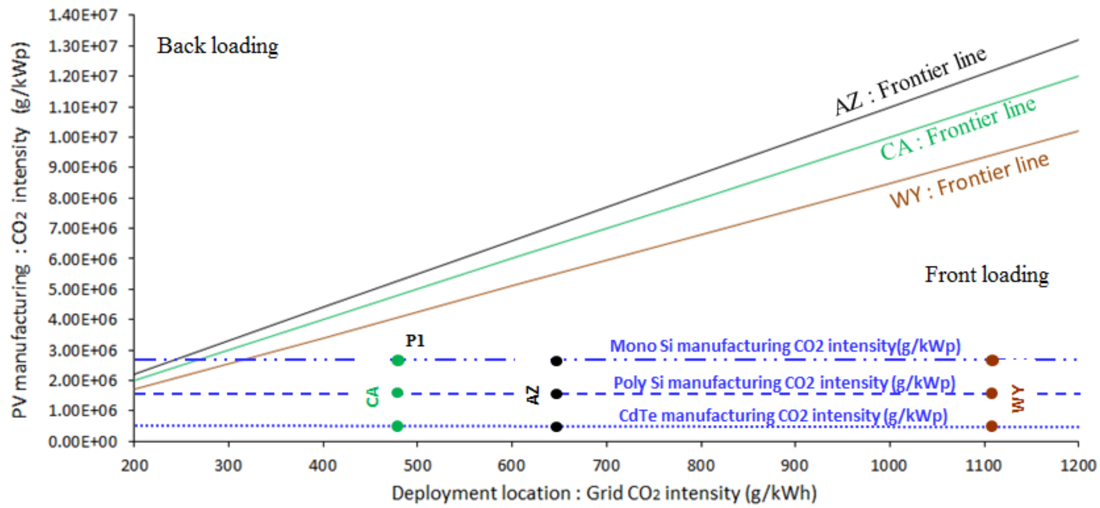

Figure 5 Optimal PV deployment strategy for minimized CRF impact. The Y-axis represents the CO_2 intensity (g/kWp) of manufacturing PV modules and X-axis represents the grid CO_2 intensity (g/kWh) at the deployment location. Frontier lines separate the plot into two optimal deployment strategy zones. The optimal deployment strategy is decided by plotting the CO_2 intensity of manufacturing energy (Y value) and the grid CO_2 intensity at the deployment location (X value) on the graph. If the plotted point is above the frontier line then back loading is the optimal strategy else front loading is the optimal strategy. The three blue lines depict the CO_2 intensity of manufacturing mono Si, Poly Si (in China) and CdTe (in Malaysia). For example, consider a scenario where PV targets in California are met by importing only mono Si modules from China. The intersection is at the point 'P1'. The frontier line for this scenario is the solid green line. This corresponds to a front loading strategy as this point lies below the solid green frontier line. Front loading is the optimal strategy for when modules manufactured in China (mono and

poly Si) or Malaysia (CdTe) are deployed in California, Wyoming or Arizona. These are depicted by the nine points

Since Mono Si is the most CO_2 intensive and CdTe is the least CO_2 intensive to manufacture among the three technologies, the CO_2 intensity of manufacturing a PV deployment mix that relies on all the three technologies will be represented by a horizontal line lying between the blue lines for Mono Si and CdTe, respectively. Front loading will be the preferred strategy across all the three states for any technology mix since the PV manufacturing CO_2 intensity line for the technology mix will lie below the blue line for Mono Si. The frontier line for Arizona is above that of California and Wyoming as the solar irradiation in Arizona is the highest (assumptions in Table 2) and this increases the PV electricity generation and the grid electricity CO_2 that is displaced. Therefore, for the same PV capacity that is deployed, the probability of Front Loading being the favorable strategy in Arizona is higher when compared to the other two states. This is reflected in the increased area covered by the front loading region for Arizona when compared to the other 2 states.

The results in Figure 5 depicts only the optimal deployment strategy and does not depict CO_2 flows and corresponding CRF impacts for the optimal front loading strategy. Five scenarios were created for each of the three states and the results were plotted to depict the difference in the net CRF benefits and CO_2 flows for PV deployments in Arizona, Wyoming and California for different deployment strategies with different technology mixes. Figure 6 and Figure 7 contain only seven scenarios that sufficiently explain all the trends observed in CO_2 flows and the corresponding CRF impacts. These trends are applicable to all the fifteen scenarios depicted in Figure 9 and Figure 10

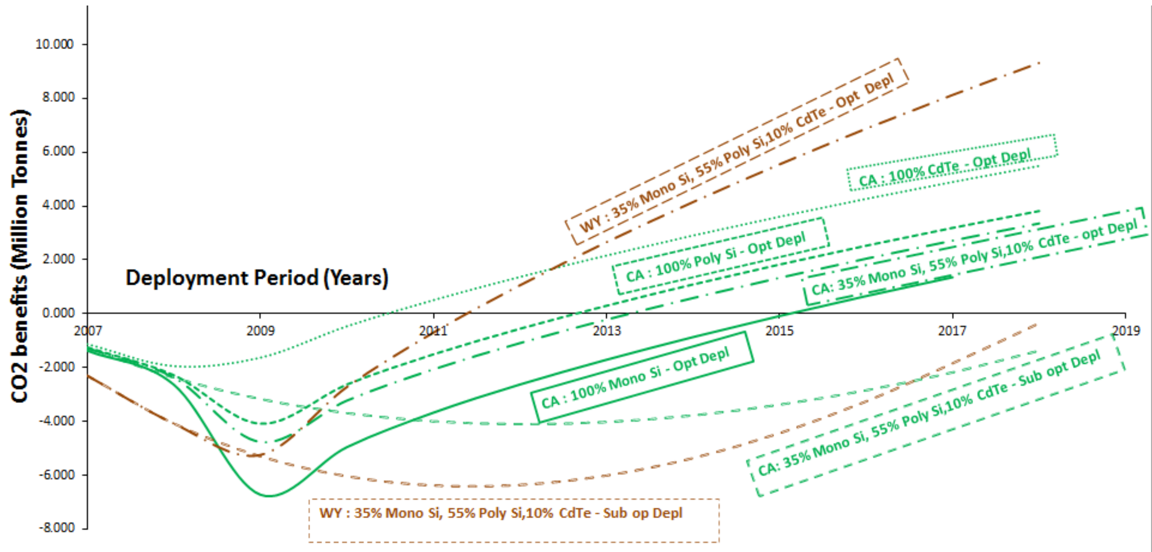

Figure 6 CO_2 benefits of PV deployments in California and Wyoming. This graph plots CO_2 benefits of PV deployments over the deployment time horizon (2007 - 2017). The manufacturing emissions and emissions due to the continued reliance on fossil fuels (in the case of sub-optimal strategy) are the CO_2 costs of PV deployments. The CO_2 avoided when PV electricity offsets grid electricity represents the CO_2 benefit. If the curve is below the X axis then CO_2 costs exceed CO_2 benefits. If the curve is above the X axis CO_2 benefits exceed the CO_2 cots. In optimal deployment (front loading for all the three states), 81MW and 169 MW are deployed in 2007 and 2008 and the remaining capacity of 1689 MW is deployed in 2009. For sub-optimal deployment, 81MW and 169 MW are deployed in 2007 and 2008 and the remaining capacity of 1689 MW is equally deployed between 2009 and 2016. Carbon payback occurs when the curve crosses the X axis. For example, in the "CA: 100% Mono Si – Opt Depl" scenario CO_2 payback occurs between 2014 and 2015.

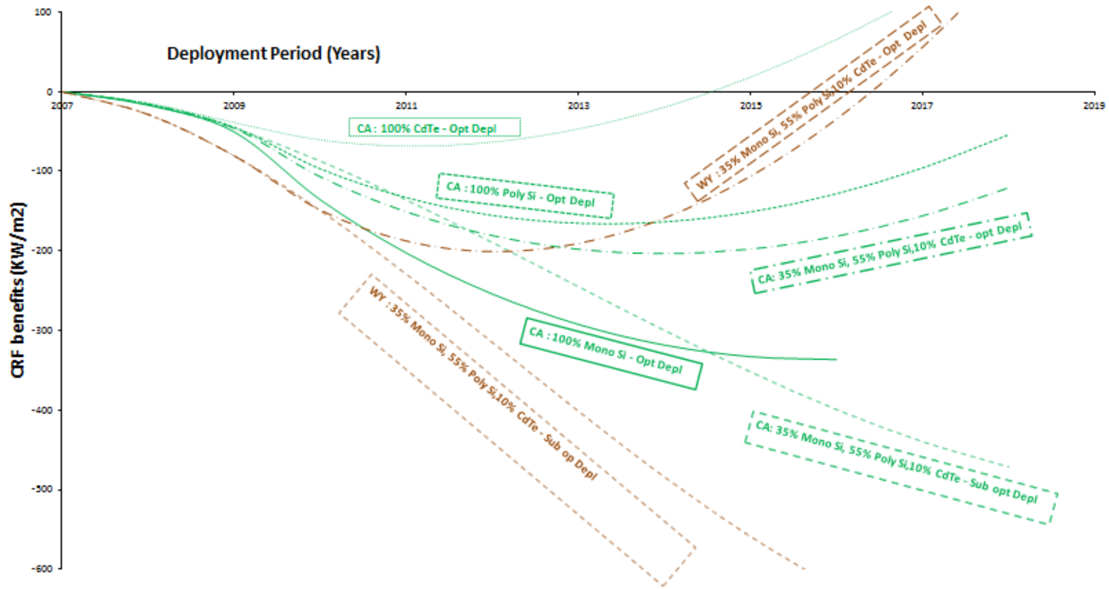

Figure 7 CRF benefits of PV deployments in California and Wyoming. This graph plots the CRF benefits of PV deployments over the deployment time horizon (2007 - 2017). CRF impacts of manufacturing emissions and emissions due to the continued reliance on fossil fuels (in the case of sub-optimal strategy) represent PV CRF costs. The CRF impacts that are avoided when PV electricity offsets grid electricity represent the CRF benefits. If the curve is below the X axis then CRF costs exceed CRF benefits of deploying the PV module. If the curve is above the X axis then CRF benefits exceed CRF costs of deploying the PV module. The optimal and sub-optimal deployment strategies are the same as in Figure 6. CRF payback occurs when the curve crosses the X axis. For example, in the "CA: 100% Poly Si – Opt Depl" scenario CRF payback occurs in 8 years. In case of sub-optimal staggered deployment scenarios ("CA: 35% Mono Si, 55% Poly Si, 100% CdTe – Sub Opt Depl"), the CRF costs increases as the grid continues to rely on fossil fuel based

electricity. This increases the CRF payback time when compared to the corresponding optimal deployment strategies

From Figure 6 and Figure 7 it can be observed that CRF payback times greater than CO_2 payback times. For example, “WY: 35% Mono Si, 55% Poly Si, 100% CdTe – Opt Depl” WY has a CO_2 pay-back time of 4 to 5 years (Figure 6) and a CRF payback time of 9 years (Figure 7). CO_2 payback times are calculated based on the magnitude of CO_2 emitted and avoided whereas CRF payback is sensitive to both the magnitude and the residence time of CO_2 in the atmosphere. While calculating the CRF payback time, earlier manufacturing emissions are weighted more than the later emissions that are avoided (refer Figure 1). For CO_2 payback times, the same weights are allocated to manufacturing CO_2 emissions irrespective of the timing. Therefore, the impact attributed to manufacturing emissions is higher when calculating the CRF payback time than when calculating the CO_2 payback time. This increases the payback time required to offset the CRF impacts of manufacturing CO_2 emissions. Also, only 2 scenarios have a net positive CRF benefit within 10 years in spite of 5 scenarios having a net positive CO_2 benefit within 10 years in Figure 6.

The CO_2 flows and CRF impacts are dependent on the CO_2 intensity of the grid electricity being displaced at the deployment location. For higher grid CO_2 intensities at the deployment location PV electricity will displace more CO_2 from the grid. This increases the avoided CO_2 benefits and therefore decreases CO_2 and CRF payback times. The CO_2 and CRF payback times for Wyoming are less than California (“WY” and “CA” scenarios in Figure 6 and Figure 7) as the CO_2 intensity of the avoided electricity in

Wyoming is higher than in California (DGI California and DGI Wyoming in Table 2). An earlier CO_2 and CRF payback implies that the CO_2 and CRF benefits for all the Wyoming strategies are higher than the corresponding strategies in California for a 10 year time frame.

The choice of PV technology to meet targets influences the CO_2 and CRF impacts. Among the three strategies “CA: 100% Mono Si – Opt Depl”, “CA: 100% Poly Si – Opt Depl”, “CA: 100% CdTe – Opt Depl” for California, the 100% CdTe mix has the highest CO_2 and CRF benefits and the earliest CO_2 and CRF break even time because CdTe has the lowest upfront manufacturing CO_2 emissions among the three technologies (MCImalayisa cdte, MCIchina poly Si, MCIchina mono Si in Table 2). Thus, in the current state of technology PV mixes that rely more on thin film CdTe and poly Si will have lower environmental impacts when compare to mono Si modules.

The CO_2 displaced and CRF impacts are dependent on the optimal rate of PV capacity addition. For the sub-optimal staggered deployment strategy, the grid continues to rely on electricity that is generated from fossil fuels. The CO_2 emissions due to continued reliance on fossil fuel electricity are greater than benefits of reduced CO_2 emissions resulting from manufacturing process improvements overtime. The optimal front-loading strategy yields greater CRF benefits as it avoids grid electricity emissions. This can be inferred from Figure 5 and Figure 6 as optimal PV deployment strategies have a shorter CO_2 and CRF payback time than sub-optimal PV deployment strategies.

Sensitivity Analysis

To analyze the changes in net CRF impacts when the factors depicted in Figure 2 are varied, this study conducted a sensitivity analysis. The relative impacts of various supply chain and PV technology factors on CRF is depicted in the results shown in Figure 8

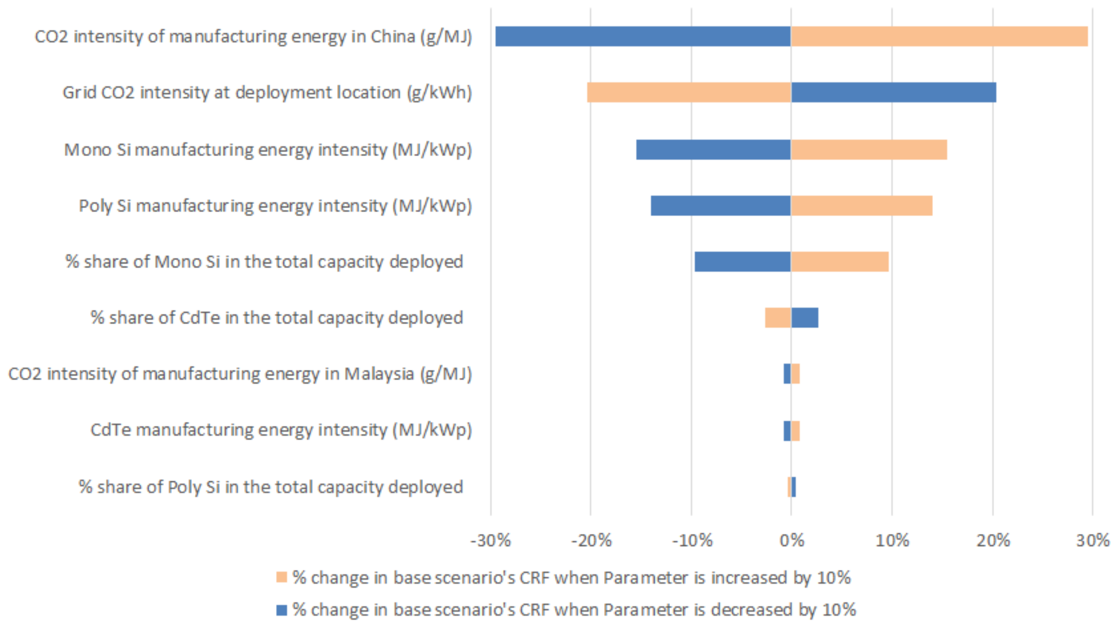

Figure 8 Sensitivity analysis for the factors influencing CRF impacts. For the base scenario, capacities of 81, 169 and 1690 MW were deployed in California in 2007,2008 and 2009 respectively with a technology mix of 35% Mono Si, 55% Poly Si and 10% CdTe. This technology mix is based on a worldwide market share of 30 to 40% for mono Si, 50 to 60% for Poly Si and 6 to 10% for CdTe from 2004 to 2010 [28]. China was the manufacturing location for Si technologies and Malaysia for CdTe and the CRF was measured over a 10 year period. The base scenario's CRF value is represented by the vertical line passing through zero. After recording the base scenario CRF, 9 runs were conducted by increasing and decreasing each variable by 10% of it's base condition value while keeping the other 8 variables

constant. CRF values for each of the 9 runs were recorded and plotted as a percentage change from the base condition CRF.

CRF impacts are most sensitive to the CO_2 embedded in the manufacturing energy in China and the manufacturing energy requirements of Poly and Mono Si modules. This is due to the 90% share of poly and mono Silicon technology in the PV capacity deployed and China's current dominant position in the crystalline PV manufacturing sector. The grid CO_2 intensity at the deployment location is the second most significant factor influencing CRF impacts. This implies that the choice of deployment location and the CO_2 intensity of the grid electricity avoided significantly influence the net environmental impacts. The third and fourth most significant factors that influence CRF imply that the use of less energy intensive PV manufacturing processes and increasing the energy and material efficiencies of manufacturing Si modules will reduce CRF impacts. The energy required to manufacture a unit area of Mono Si models has decreased by only 6% from 2006 to 2011 ([29],[30]). A decrease in the energy requirements of upstream metallurgical refining processes that contribute around 60% an 79% of the total energy footprint for mono Si modules [30] will reduce CRF impacts and manufacturing costs.

Discussion

Future deployments of PV modules, manufactured predominantly in coal dependent China, will have significant manufacturing CO_2 emissions. PV capacity additions have shown a steep increase and two-thirds of the all the historical PV capacity ever deployed were added only after January 2011 [31]. PV system production has increasingly shifted to China which is dependent on fossil fuels for manufacturing activities. China's share in the world poly-silicon and module manufacturing markets has increased to 30% and 63%, respectively [32] and coal contributes to around 67% of China's primary energy mix [33]. Existing PV LCAs do not provide methods to measure time sensitive short-term CRF impacts of large scale PV manufacturing in CO_2 intense grid locations and therefore cannot evaluate the warming potential of rapid PV deployments over 30 to 50 year time frames defined by climate policy to prevent a global temperature increase. This study has provided a framework evaluate the time sensitive warming impacts of CO_2 flows during the PV lifecycle and has also demonstrated that CRF payback times are longer than CO_2 payback times. Also, under certain scenarios CRF increases over a period of 10 years in spite of the benefits of CO_2 avoided being greater than the PV system's life cycle CO_2 footprint.

The results have shown that dynamic CRF impacts can be minimized by the choice of PV technology, energy mixes at the deployment and manufacturing locations and the rate of deployment. The environmental benefits over a period of ten years increase with aggressive deployment strategies when higher PV capacities are deployed earlier on in California, Wyoming and Arizona. The benefits are higher in states that have a greater reliance on fossil fuels for their electricity mix as PV displaces more CO_2 intense electricity. Also, PV mixes that have higher shares of CdTe and Poly Si PV modules have increased CRF benefits as these technologies have lower manufacturing energy requirements when compared to Mono Si.

The novel framework contained in this study informs policy makers and PV manufacturers on strategies to minimize radiative forcing impacts and identify environmental hot-spots in the PV manufacturing lifecycle. A reduction in the energy requirements for upstream metallurgical processes for solar grade silicon and a reduction in poly-Silicon wastage while manufacturing PV cells will significantly decrease the CRF impacts over the PV life-cycle for future capacity additions.

While this framework was applied to PV system deployments, it can also be extended to evaluate the short term CRF impacts for other renewable energy (RE) systems. RE systems are essentially CO_2 offsetting mechanisms with initial CO_2 invested in manufacturing being recovered gradually over time when the RE systems displaces electricity generated from fossil fuels. After identifying the relevant supply chain and technology parameters for the RE system, this framework can be integrated with LCAs to provide the time sensitive CO_2 and CRF impacts

REFERENCES

1. Masson, G., M. Latour, and D. Biancardi, Global market outlook for photovoltaics until 2016. European Photovoltaic Industry Association, 2012.

2. Media, G.T. GTM Research: Yingli Gains Crown as Top Producer in a 36 GW Global PV Market. 2013; Available from: http://www.greentechmedia.com/articles/read/Yingli-Gains-Crown-As-Top-Producer-in-a-36-GW-Global-PV-Market.

3. DOE, U., Sunshot Vision Study. US DOE, Washington, DC, 2012.

4. IEA, Technology Roadmap: Solar photovoltaic energy, 2010.

5. DOE, 2010 Solar Technologies Market Report, 2011.

6. Drury, E., P. Denholm, and R.M. Margolis, The solar photovoltaics wedge: pathways for growth and potential carbon mitigation in the US. Environmental Research Letters, 2009. **4**(3): p. 034010.

7. UNEP, The Emissions Gap Report 2012, 2012.

8. Iso, I., 14040 Environmental management-life cycle assessment-principles and framework. London: British Standards Institution, 2006.

9. Peng, J., L. Lu, and H. Yang, Review on life cycle assessment of energy payback and greenhouse gas emission of solar photovoltaic systems. Renewable and Sustainable Energy Reviews, 2013. **19**: p. 255-274.

10. Alsema, E., Energy pay-back time and CO2 emissions of PV systems. Progress in photovoltaics: research and applications, 2000. **8**(1): p. 17-25.

11. Fthenakis, V. and E. Alsema, Photovoltaics energy payback times, greenhouse gas emissions and external costs: 2004–early 2005 status. Progress in photovoltaics: research and applications, 2006. **14**(3): p. 275-280.

12. Hsu, D.D., et al., Life cycle greenhouse gas emissions of crystalline silicon photovoltaic electricity generation. Journal of Industrial Ecology, 2012. **16**(s1): p. S122-S135.

13. Kim, H.C., et al., Life Cycle Greenhouse Gas Emissions of Thin-film Photovoltaic Electricity Generation. Journal of Industrial Ecology, 2012. **16**(s1): p. S110-S121.

14. Kato, K., et al., A life-cycle analysis on thin-film CdS/CdTe PV modules. Solar Energy Materials and Solar Cells, 2001. **67**(1): p. 279-287.

15. Fthenakis, V., et al., Methodology guidelines on life cycle assessment of photovoltaic electricity. IEA PVPS Task, 2011. **12**.

16. Held, M. and R. Ilg, Update of environmental indicators and energy payback time of CdTe PV systems in Europe. Progress in photovoltaics: research and applications, 2011. **19**(5): p. 614-626.

17. Fthenakis, V.M., H.C. Kim, and E. Alsema, Emissions from photovoltaic life cycles. Environmental science & technology, 2008. **42**(6): p. 2168-2174.

18. Pachauri, R. and A. Reisinger, IPCC fourth assessment report. IPCC, Geneva, 2007.

19. Kendall, A. and L. Price, Incorporating time-corrected life cycle greenhouse gas emissions in vehicle regulations. Environmental science & technology, 2012. **46**(5): p. 2557-2563.

20. Kendall, A., B. Chang, and B. Sharpe, Accounting for time-dependent effects in biofuel life cycle greenhouse gas emissions calculations. Environmental science & technology, 2009. **43**(18): p. 7142-7147.

21. Kendall, A., Time-adjusted global warming potentials for LCA and carbon footprints. The International Journal of Life Cycle Assessment, 2012. **17**(8): p. 1042-1049.

22. Chang, B. and A. Kendall, Life cycle greenhouse gas assessment of infrastructure construction for California's high-speed rail system. Transportation Research Part D: Transport and Environment, 2011. **16**(6): p. 429-434.

23. FirstSolar, Life Cycle Carbon Impacts of Utility Scale Photovoltaic Projects, 2011.

24. Commission, C.P.U. California Solar Initiative. 2012 [cited 2013; Available from: http://www.cpuc.ca.gov/puc/energy/solar/aboutsolar.htm.

25. Commission, C.E. California Solar Photovoltaic Statistics & Data. 2013 [cited 2013; Available from: http://energyalmanac.ca.gov/renewables/solar/pv.html.

26. PVTECH. Top 10 PV module suppliers in 2012. 2012 [cited 2013; Available from: http://www.pv-tech.org/guest_blog/top_10_pv_module_suppliers_in_2012.

27. Personal Communication with First Solar, 2013.

28. FRAUNHOFER, Photovoltaics Report - Fraunhofer institute for solar energy systems, 2012.

29. Fthenakis, V., et al. Update of PV energy payback times and life-cycle greenhouse gas emissions. in 24th European Photovoltaic Solar Energy Conference and Exhibition. 2009.

30. Wild-Scholten, M.J.M.d., Energy payback time and carbon footprint of commercial photovoltaic systems. Solar Energy Materials and Solar Cells, 2013. **119**: p. 296-305.

31. GreenTechMedia. 2/3rds of Global Solar PV Has Been Installed in the Last 2.5 Years. 2013 [cited 2013; Available from: http://www.greentechmedia.com/articles/read/chart-2-3rds-of-global-solar-pv-has-been-connected-in-the-last-2.5-years.

32. IEA, National Survey Report of PV Power Applications in China 2012.

33. IEA, Facing China's Coal Future: Prospects and Challenges for Carbon Capture and Storage, 2012.

34. Simparo, Grid CO2 intensity as reported by Simparo. 2013.

35. NREL. National Solar Radiation Data Base - Class I locations. 2010; Available from: http://rredc.nrel.gov/solar/old_data/nsrdb/1991-2010/hourly/list_by_state.html#C.

36. EIA. Transmission and Distribution losses in the United States. 2012 [cited 2013; Available from: http://www.eia.gov/tools/faqs/how-much-electricity-lost-transmission-and-distribution-united-states.

37. DOE, U. State Electrcity Profiles. 2012 [cited 2013; Available from: http://www.eia.gov/electricity/state/.

38. EPA, EPA Analysis of the American Clean Energy and Security Act of 2009, 2009.

APPENDIX A

CALCULATION OF CRF WEIGHTS FOR CO_2 EMISSIONS

A	B	C	D	E
Atmospheric residence time (years)	CO_2 remaining in the atmosphere after sequestration (Kgs)	Radiative Forcing (watt/m2)	CRF weight (watt/m2)	CRF weight allocated to emission occurring in year
1	0.874774431	1.24E-05	1.24E-05	10
2	0.810850811	1.15E-05	2.38E-05	9
3	0.773796358	1.09E-05	3.48E-05	8
4	0.748767683	1.06E-05	4.53E-05	7
5	0.729352906	1.03E-05	5.57E-05	6
6	0.712769869	1.01E-05	6.57E-05	5
7	0.697799641	9.86E-06	7.56E-05	4
8	0.683897154	9.67E-06	8.53E-05	3
9	0.670808408	9.48E-06	9.47E-05	2
10	0.658405688	9.31E-06	1.04E-04	1

Table 1 Calculation of CRF weights for CO_2 emissions

Column B values are calculated by substituting 't' (in equation (1)) with the corresponding Column A values. Column C values are calculated by multiplying the corresponding column B values by a_c, the radiative efficiency of CO_2 (assumed to be constant at 1.4135×10^{-5}) . Column D values are the cumulative sum of column C values until that year. The weights in column D are assigned to CO_2 emissions according to the residence time in the atmosphere. For example, over a 10 year horizon an emission in year 7 has an atmospheric residence time of 3 years and is therefore assigned a CRF weight of 4.53E-05. This allocation of weighting factors is shown in column E.

APPENDIX B

CO_2 AND CRF PAYBACK TIMES IN CALIFORNIA, ARIZONA AND WYOMING

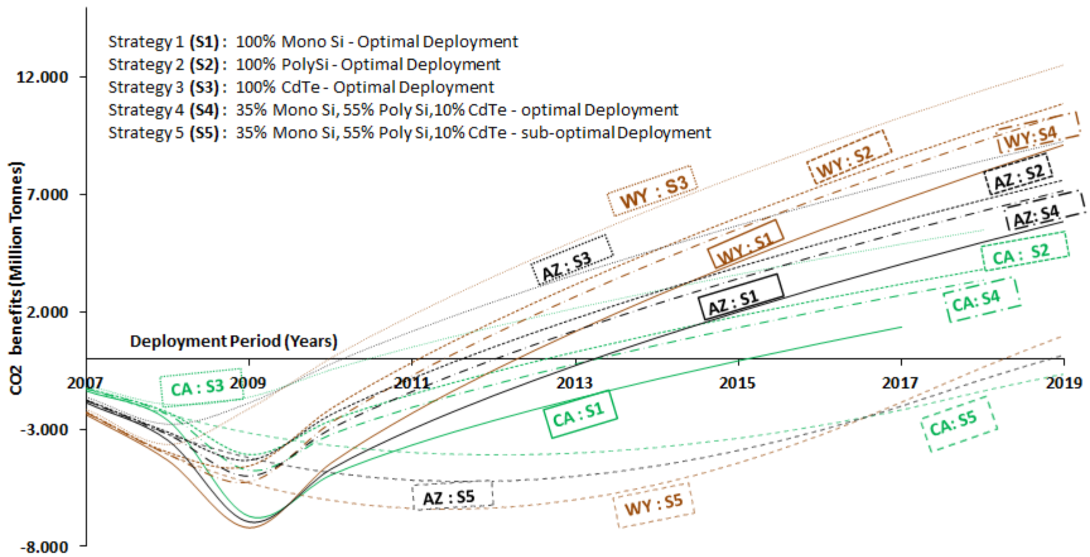

Figure 9 CO_2 payback times for all scenarios in CA, AZ and WY. In optimal deployment, 81MW and 169 MW are deployed in 2007 and 2008 and the remaining capacity of 1689 MW is deployed in 2009. For sub-optimal deployment, 81MW and 169 MW are deployed in 2007 and 2008 and the remaining capacity of 1689 MW is equally deployed between 2009 and 2016.

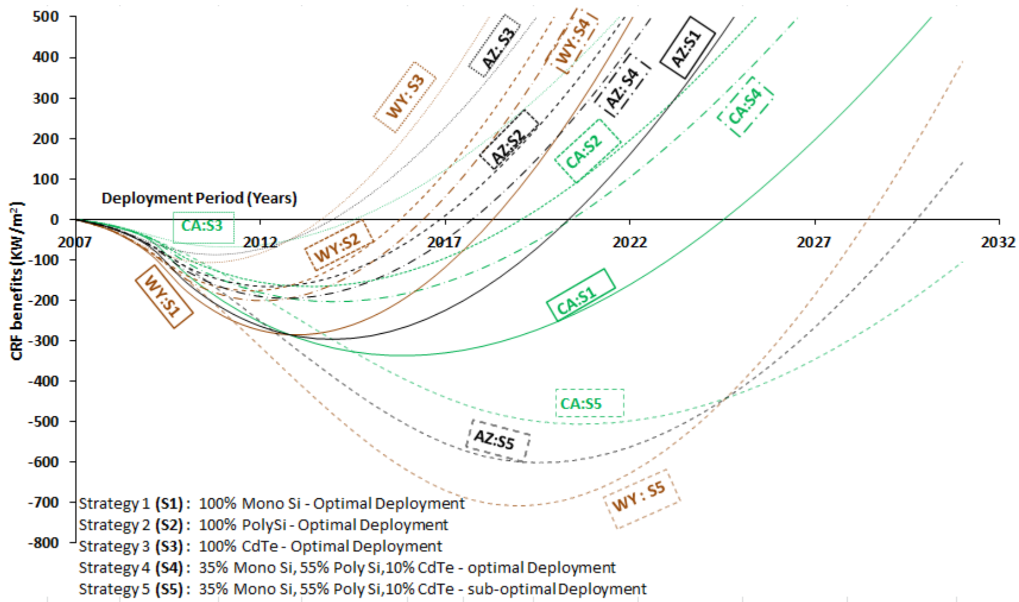

Figure 10 CRF payback times for all scenarios in CA, AZ and WY. Optimal deployment and sub-optimal deployments are the same as in Figure 9

APPENDIX C

DATA ASSUMPTIONS

The MCI_{china} value for Mono and Poly Si PV technologies in 2011 is the base value. MCI is directly proportional to the manufacturing energy (ME) embedded in the PV module (MJ/m2) and inversely proportional to the efficiency (eff) of the module. To get the MCI_{china} values for any other year 't' between 2007 and 2017, the base MCI_{china} value is multiplied by the ratios (ME_t/ME_{2011}) and (eff_{2011}/eff_t) . The degradation in the module performance over time is assumed to be 0.7%/year [30]. The following are the values used in the optimization framework

Parameter	Value	Used in Equation	Source
$MCI_{china\ mono\ Si}$ in 2011	2870000 (g/kWp)	(4)	[30].
$MCI_{china\ poly\ Si}$ in 2011	1590000 (g/kWp)	(4)	[30]
$MCI_{malayisa\ for\ CdTe}$ in 2011	498000 (g/kWp)	(4)	[30] has reported a value of 630000 g/ kWp based on manufacturing conditions in China. This value has been multiplied by a ratio of the current grid mixes in Malaysia (909 g/kWh from [34]) and China (1148 g/kWh from [34]) as CdTe is assumed to be manufactured in Malaysia.
DGI California	481 (g/kWh)	(5),(6)	[34]
DGI Arizona	644(g/kWh)	(5),(6)	[34]
DGI Wyoming	1105 (g/kWh)	(5),(6)	[34]
pr	0.75	(5),(6)	[15]
Irr Arizona	2200 (kwh/m2 year)	(5),(6)	[35]
Irr California	2000 (kwh/m2 year)	(5),(6)	[35]
Irr Wyoming	1700 (kwh/m2 year)	(5),(6)	[35]
op	.1	(5),(6)	[23]
tl	.07	(5),(6)	[36]

Table 2 Values of parameters used for optimizing PV deployment strategy for minimal CRF impacts

The CO_2 emissions per kWh of electricity produced at California, Arizona and Wyoming have not shown a consistently increasing or decreasing trend from 2001 to 2009 [37]. An annual decrease of 2% has been assumed for the period from 2007 to 2016 for these three destination locations. This annual decrease is comparable to the 17% GHG emission reductions mandated by the American Climate and Energy Security Act for the period between 2005 and 2020 [38].